

# $\sigma$ -Aromaticity in $H_3^+$ and $Li_3^+$ : Insights from ring-current maps

Remco W.A. Havenith<sup>a,\*</sup>, Frank De Proft<sup>b</sup>, Patrick W. Fowler<sup>c,1</sup>, Paul Geerlings<sup>b</sup>

<sup>a</sup> Debye Institute, Theoretical Chemistry Group, Utrecht University, Padualaan 8, 3584 CH Utrecht, The Netherlands

<sup>b</sup> Eenheid Algemene Chemie (ALGC), Vrije Universiteit Brussel (VUB), Faculteit Wetenschappen, Pleinlaan 2, 1050 Brussels, Belgium

<sup>c</sup> Department of Chemistry, University of Exeter, Stocker Road, Exeter EX4 4QD, UK

Received 11 March 2005; in final form 21 March 2005

Available online 14 April 2005

## Abstract

Putative  $\sigma$ -aromaticity of the clusters  $H_3^+$  and  $Li_3^+$  is investigated by computation of ring-current maps in the ab initio ipsocentric approach. Although  $H_3^+$  shows a marked diatropic ring-current and can be considered  $\sigma$  aromatic on the magnetic criterion,  $Li_3^+$  shows no global current and is non-aromatic on this criterion, in spite of its electron count and negative NICS value. The difference in magnetic response is interpreted in terms of orbital energies using the ipsocentric model: in  $Li_3^+$  the diatropic HOMO–LUMO excitation is opposed by paratropic excitations to higher unoccupied orbitals; in  $H_3^+$  this cancellation does not occur.

© 2005 Elsevier B.V. All rights reserved.

## 1. Introduction

$\sigma$ -Aromaticity has long been invoked in the description of the electronic structure of cyclopropane and related organic ring systems [1–4], and recently entered inorganic chemistry through the debate over the aromaticity of all-metal aromatics such as  $Al_4^{2-}$  [5], and valence-isoelectronic analogues  $Ga_4^{2-}$  [6] and  $Hg_4^{2-}$  [7]. The species  $Al_4^{2-}$  was initially described as  $\pi$ -aromatic purely on the basis of its count of two  $\pi$ -electrons [5], but examination of its ring-current [8,9] indicated that the  $\pi$ -electrons were magnetically inactive, and that a diatropic current arose from the  $\sigma$  system, so that this molecule should rather be considered  $\sigma$ -aromatic. Assignments of combined  $\sigma$  and  $\pi$  aromaticity have also been proposed [10], and even of a three-fold  $\pi$  plus double  $\sigma$  aromaticity [11], though the lack of  $\pi$  ring-current remains an objection to this view according to the magnetic criterion of aromaticity. Ring-current studies on

four- $\pi$  analogues, which exhibit a mixture of diatropic and paratropic circulations, gave further weight to the view that  $\pi$  electron-counting rules do not always suffice for all-metal systems [12].

Recently, Alexandrova and Boldyrev [13] investigated  $\sigma$ -aromaticity and antiaromaticity of small alkali/alkaline-earth metal clusters. A conclusion, based on energetics evaluated from a series of homodesmotic reactions, on orbital topology, and on simple electron count, was that  $Li_3^+$  should be considered  $\sigma$ -aromatic. The equilateral triangular geometry of  $Li_3^+$  was found to be the global minimum on the potential energy surface. In the same study,  $Li_3^-$  was found to have similarities in orbital topology to antiaromatic cyclobutadiene, and to undergo Jahn–Teller distortion from the  $D_{3h}$  high-symmetry point, as expected for an antiaromatic system. Electron counting arguments allow for the coexistence of  $\sigma$  antiaromaticity with  $\pi$  aromaticity, as Boldyrev and Wang [14] point out in connection with a compound synthesised by Twamley and Power [15].

Geometry, energetics and electron count aside, an independent definition of aromaticity is the ability of a molecule to sustain a diatropic ring current [16–20]. This property can be probed by direct calculation of

\* Corresponding author. Fax: +31 30 253 7504.

E-mail address: [r.w.a.havenith@chem.uu.nl](mailto:r.w.a.havenith@chem.uu.nl) (R.W.A. Havenith).

<sup>1</sup> Address from 1 August 2005, Department of Chemistry, University of Sheffield, Sheffield S3 7HF, UK

magnetic-field induced current density at the ipsocentric Hartree–Fock level [21–24], an ab initio approach that lends itself to visualisation and physical interpretation in terms of orbital contributions governed by symmetry rules [25,26]. The ring-current criterion has not so far been applied directly to  $\text{Li}_3^+$ . The present study addresses the question of whether  $\text{Li}_3^+$  is aromatic on the magnetic criterion. Comparison of current density maps is made for  $\text{Li}_3^+$ ,  $\text{H}_3^+$ , and the two-centre systems  $\text{Li}_2$  and  $\text{H}_2$ , with analysis of the maps in terms of the different electronic structures of Li–Li and H–H bonds. The maps also provide an interpretation of the computed values of nucleus independent chemical shifts (NICS), which are often taken as indicators of magnetic aromaticity, even though their relationship to existence of a ring current is indirect. In contrast with the inference from the simple electron-counting approach, and despite a large and negative NICS value,  $\text{Li}_3^+$  is found to have no significant global diatropic ring-current arising from its two  $\sigma$  valence electrons.  $\text{Li}_3^+$  is therefore (magnetically) non-aromatic.  $\text{H}_3^+$ , on the other hand, qualifies for the description of  $\sigma$ -aromatic by virtue of its global diatropic ring-current.

## 2. Computational details

Magnetic response properties were studied for  $\text{Li}_3^+$ ,  $\text{H}_3^+$ ,  $\text{Li}_2$ , and  $\text{H}_2$ . Geometries were optimised at the MP2/6-311G\*\* level using the GAMESS-UK program [27]. At this level of theory, optimised bond lengths are 3.001 Å for  $\text{Li}_3^+$ , 0.874 Å for  $\text{H}_3^+$ , 2.736 Å for  $\text{Li}_2$ , and 0.738 Å for  $\text{H}_2$ . Current-density maps were computed at the coupled Hartree–Fock level in the same basis using the distributed-origin methods of Keith and Bader [21,22], as developed by the Modena group [23,24] and implemented in the SYMO program [28]. The diamagnetic zero (DZ) variant of continuous transformation of origin of current density (CTOCD), where the current density at each point in space is calculated with that point as origin, was used for the main maps. This *ipsocentric* choice of vector potential provides a uniquely simple partition of the first-order wavefunction, and hence of the induced current density, into physically non-redundant orbital contributions that involve only occupied-to-unoccupied orbital transitions and obey simple symmetry-based selection rules for diamagnetic (diatropic) and paramagnetic (paratropic) current [25] (the terms diamagnetic and paramagnetic describe the circulation by comparing its sense to the classical Larmor circulation; diatropic and paratropic, often used as synonyms, refer to its effect on chemical shift of a real or fictitious  $^1\text{H}$  nucleus in an exo-bond). In the maps, current densities induced by a magnetic field of unit strength acting perpendicular to the plane of the nuclei are plotted in that plane, with contours showing the

magnitude of current density and vectors its magnitude and direction. In all plots, diamagnetic (diatropic) circulation is counter-clockwise. As a check on the reliability of the CTOCD–DZ method in a plane that contains nuclei [29], the induced current density of  $\text{Li}_3^+$  was also computed using the CTOCD–PZ2 [24] method.

Schematic energy-level diagrams were derived from the RHF orbital energies in order to illustrate the operation of the selection rules. To indicate the effects of the mapped currents on integrated molecular properties, NICS values were calculated at ring centres (NICS(0)) and at heights of 0.5 and 1 Å, using the CTOCD–PZ2 approach [30]. Contour plots of HOMOs of both  $\text{H}_3^+$  and  $\text{Li}_3^+$ , were also constructed to aid interpretation of the contribution of this orbital to induced current density.

## 3. Results and discussion

Fig. 1a shows the main result of our study. The  $\text{Li}_3^+$  system exhibits *no* significant ring current, and must therefore be considered non-aromatic (and in particular non- $\sigma$ -aromatic) on the magnetic criterion. This is in spite of a two electron count in the valence  $\sigma$  system. CTOCD–DZ and CTOCD–PZ2 maps (Figs. 1a and c) are essentially indistinguishable outside the immediate vicinity of the nuclei, showing that this lack of ring-current is not an artifact of the method but a feature of the electronic structure. The HOMO electrons in  $\text{Li}_3^+$  contribute local rather than global circulations (Fig. 1b).

In contrast, the valence-isoelectronic system  $\text{H}_3^+$  has a pronounced diatropic current that follows the ring perimeter, as Fig. 2 shows. The maximum in-plane current induced per unit magnetic field ( $j_{\text{max}}$ ) is 0.09 a.u., which compares with  $j_{\text{max}} = 0.08$  a.u. for the archetypal  $\pi$  ring-current of benzene (at a height of 1  $a_0$ , calculated at the ipsocentric 6-31G\*\* level of theory).  $\text{H}_3^+$  has two electrons in a HOMO of  $a'_1$  symmetry, as does  $\text{Li}_3^+$ , but in  $\text{H}_3^+$  they contribute a global circulation.

What then causes the difference in magnetic response? The orbital model derived from the ipsocentric approach accounts for the currents induced in a monocycle by a magnetic field perpendicular to the nuclear plane through two symmetry-based selection rules for the virtual excitations that contribute to current [25,26]. Diatropic circulations arise from those excitations from occupied to unoccupied orbitals where the product of orbital symmetries contains the symmetry of one or both the in-plane translations. Paratropic circulations arise from those excitations where the product of orbital symmetries contains the symmetry of the sole in-plane rotation. In  $D_{3h}$  symmetry, the in-plane translations transform as  $e'$  and the in-plane rotation as  $a'_2$ . In the first-order wavefunction, and hence in the current, the symmetry-allowed contributions are weighted by energy

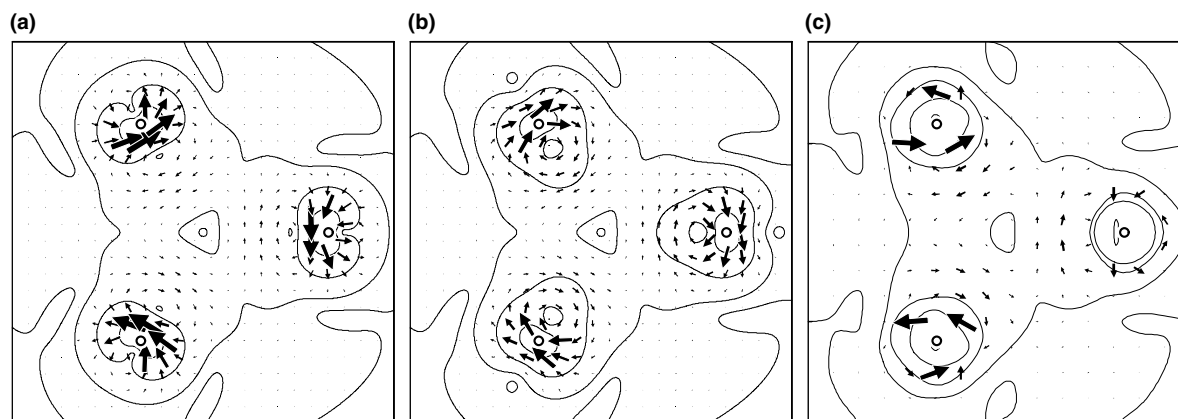


Fig. 1. Current density maps plotted in the molecular plane for  $\text{Li}_3^+$ : (a) Total current density calculated using the ipsocentric CTODC-DZ formulation, (b) HOMO ( $2a_1'$ ) contribution to the total current density, and (c) the total current density calculated using the allocentric [29] CTODC-PZ2 formulation.

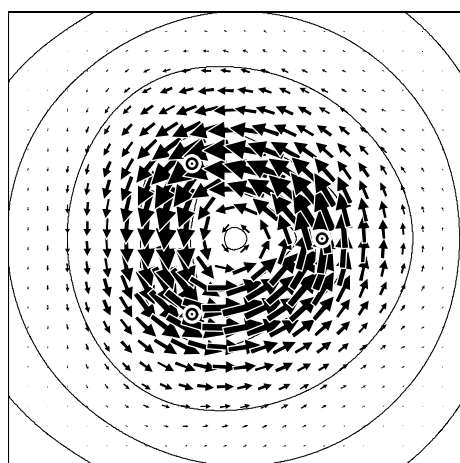


Fig. 2. Computed total current density map plotted in the molecular plane for  $\text{H}_3^+$  calculated using the ipsocentric formalism. The  $j_{\text{max}}$  value is 0.09, compared to a  $j_{\text{max}}$  of 0.08 calculated for benzene.

denominators. Fig. 3 shows the orbital energy level diagram for  $\text{Li}_3^+$  and  $\text{H}_3^+$ , with allowed transitions of both types marked.

In both cases, the HOMO is totally symmetric, and the HOMO–LUMO excitation has symmetry product  $a_1' \times e' = e'$ , corresponding to a diatropic sense of the induced current. In  $D_{3h}$  symmetry, a paratropic contribution to the HOMO current density requires an excitation to an  $a_2'$  orbital; in the present 6-311G\*\* basis, the lowest available target orbitals are the LUMO + 8 for  $\text{H}_3^+$ , and LUMO + 5 for  $\text{Li}_3^+$ . The HOMO–LUMO separations are  $1.0122 E_h$  ( $\text{H}_3^+$ ) and  $0.2390 E_h$  ( $\text{Li}_3^+$ ) at the RHF/6-311G\*\* level. The lowest unoccupied  $a_2'$  orbital of  $\text{H}_3^+$  lies at high energy, at  $2.1430 E_h$ ,  $3.3477 E_h$  above the HOMO. For  $\text{Li}_3^+$ , however, the lowest orbital of  $a_2'$  symmetry is at  $-0.0192 E_h$ , only  $0.3445 E_h$  above the HOMO. Thus, the orbital energies are already suggestive of a distinction between the two systems, with the

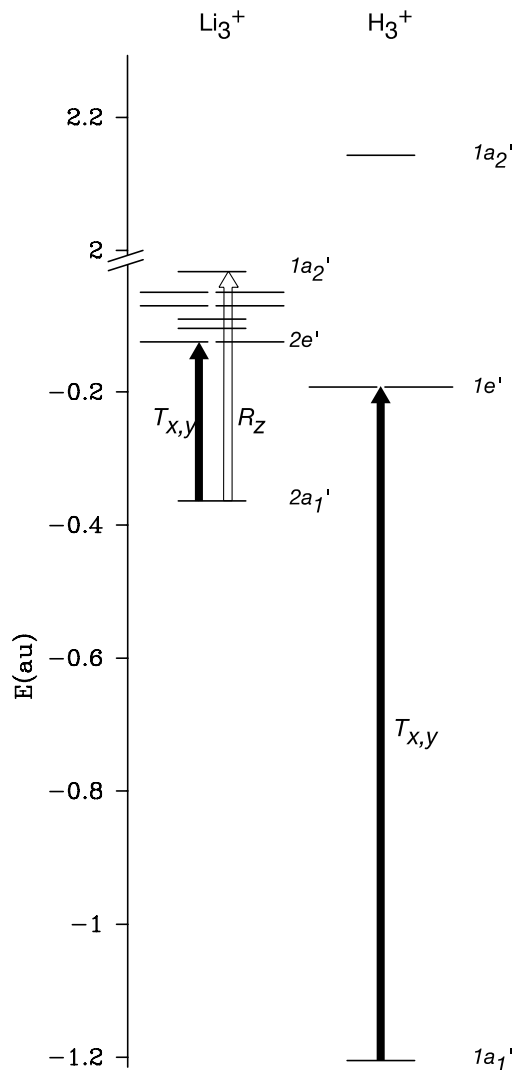


Fig. 3. Energy level diagrams and significant translationally ( $T_{x,y}$ ) and rotationally ( $R_z$ ) allowed transitions leading to the current for  $\text{H}_3^+$  and  $\text{Li}_3^+$ .

induced current in  $H_3^+$  likely to be dominated by a single excitation, but the current in  $Li_3^+$  likely to have opposing contributions.

The character of the paratropic excitations reinforces the distinction. The  $a'_1 \rightarrow a'_2$  excitation can be considered as a concerted rotation on each of the atomic centres (see also [31]). The strength of paratropic current is not determined solely by the energy gap between the occupied orbital  $\phi_i$  and unoccupied orbital  $\phi_f$ , but also by the angular-momentum matrix element that connects them. The magnitude of this matrix element can be estimated by consideration of the local atomic symmetry around the individual atoms. If  $\phi_i$  and  $\phi_f$  include atomic functions with a common orbital angular momentum (e.g., 2p orbitals), this matrix element can be expected to be large; if, on the other hand,  $\phi_i$  and  $\phi_f$  belong to shells with different angular momentum quantum number, (e.g., 1s-based  $\phi_i$  and 2p-based  $\phi_f$ ), this matrix element may be vanishingly small. Contour plots of the  $a'_1$  HOMO orbitals of  $Li_3^+$  and  $H_3^+$  (Fig. 4) show a marked difference between the two systems: whereas  $H_3^+$  has a simple, classical three-centre/two-electron bond, with mainly s-character,  $Li_3^+$  has three-centre/two-electron bond made up of sp-hybrids, leading to increased overlap between the atomic orbitals and their rotated counterparts, and thus to an enhanced matrix element of the angular momentum operator.

Thus in  $H_3^+$ , the orbital model leads us to expect a strong diatropic HOMO–LUMO contribution, uncancelled by the high-energy excitations. For  $Li_3^+$ , however, the  $e'$  and  $a'_2$  excitations are of comparable energy, and have favourable symmetry for a concerted rotation, and the observed localised HOMO current of  $Li_3^+$  is therefore rationalised as the result of cancellation between

diatropic and paratropic terms in the HOMO orbital contribution.

These clear differences in the current density maps are not reflected in the integrated property that is often used to diagnose aromaticity, the NICS value [16]. Table 1 lists NICS calculated in the PZZ approach at heights 0, 0.5, 1.0 Å above the ring centres of  $H_3^+$  and  $Li_3^+$ . Both systems exhibit large and negative NICS(0) values, dying off rapidly with height for  $H_3^+$ , more slowly for  $Li_3^+$ . Both would be assigned aromatic status on the usual NICS criterion. However, as an isotropic property, NICS contains many contributions in addition to those (if any) from the ring-current. Axial components of the shielding tensor, the only components that would be expected to reflect ring-current directly, also follow the same misleading trend, as the values NICS<sub>zz</sub> in Table 1 show. A feature which may make reliance on NICS as indicators of ring-current problematic in the present case is local electron density. When used to probe aromaticity of cycles such as benzene, NICS(0) refers to a point coinciding with a minimum in the electron density (following the nomenclature of the atoms-in-molecules (AIM) theory [32], a (3,+1) ring critical point). At the ring centres of  $Li_3^+$  and  $H_3^+$  [33], however, non-nuclear maxima ((3,−3) critical points) of the density are located. Similar maxima are also encountered in other Li clusters [34]. These maxima act like nuclei, in that an external magnetic field induces a current around such a point, as it does around a bond-critical point (see also Fig. 5 for the induced current around a (3,−1) bond-critical point in  $H_2$ , with a ‘NICS(0)’ of −32.4, but no possibility of a ring-current), but these currents do not necessarily bear any resemblance to a ring-current, which is the defining property of aromaticity. Both triatomic cluster molecules are far from the usual regime of application of NICS. Hence, probing NICS at maxima of the density may well lead to misleading conclusions about aromaticity. Consideration of the profile of NICS with distance from the molecular plane does not appear to help in the present case. An interesting critique of the NICS approach in general is given in [35].

The difference in bonding between the two triatomic clusters is already apparent in the neutral diatomics  $H_2$  and  $Li_2$ . The induced current density is plotted for these systems in Fig. 5. In the case of  $H_2$  (Fig. 5b) a  $\sigma$ -bond circulation is clearly visible, whereas for  $Li_2$  the only significant currents are those circling the nuclei, i.e., in the  $1s^2$  cores. This difference between s- and

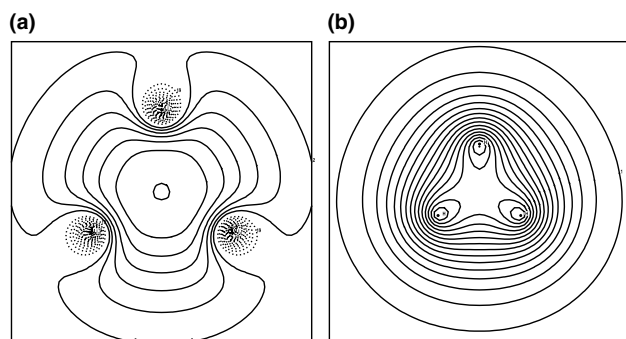


Fig. 4. Contour plots of the  $a'_1$  HOMO of (a)  $Li_3^+$ , and (b)  $H_3^+$ .

Table 1

Nucleus independent chemical shifts (ppm) for  $H_3^+$  and  $Li_3^+$  computed at the RHF/6-311G\*\* level using the CTOCD–PZZ approach [24]

Molecule	NICS(0.0)	NICS <sub>zz</sub> (0.0)	NICS(0.5)	NICS <sub>zz</sub> (0.5)	NICS(1.0)	NICS <sub>zz</sub> (1.0)
$H_3^+$	−33.6	−37.5	−13.1	−21.9	−1.9	−8.0
$Li_3^+$	−11.2	−9.2	−9.9	−8.8	−7.0	−7.5

Mean values at height  $h$  (Å) are denoted NICS( $h$ ), and out-of-plane components are denoted NICS<sub>zz</sub>( $h$ )

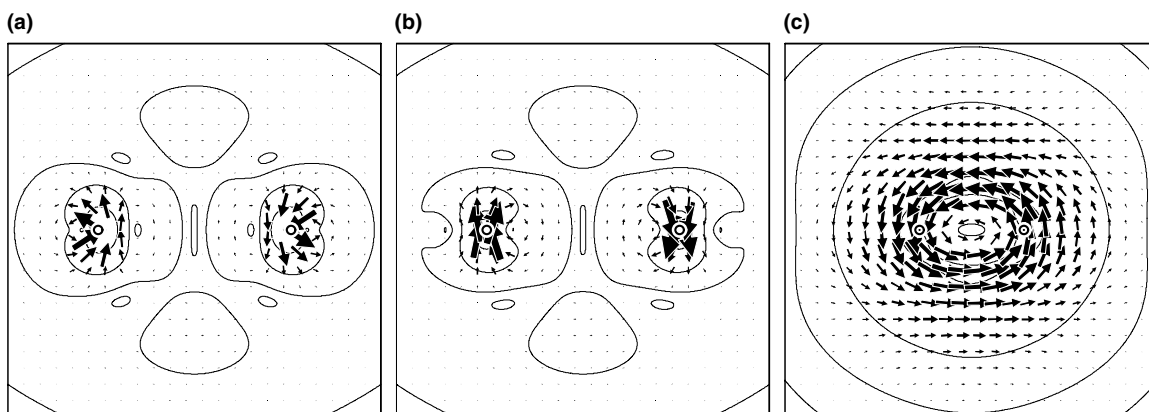


Fig. 5. Current density maps plotted in the molecular plane for (a) total current density for  $\text{Li}_2$ , (b) HOMO ( $2\sigma_g^+$ ) contribution to the total current density, and (c) total current density for  $\text{H}_2$  computed using the ipsocentric formalism.

sp-bonded systems is again explicable on grounds of accessibility of empty low-lying  $\pi_g$  orbitals in the Li-species, reached by rotationally allowed transitions, and giving rise to paramagnetic contributions that cancel the diamagnetic bond current.

#### 4. Conclusion

If the magnetic criterion is applied directly, by investigation of the ring-current, the all-metal triatomic,  $\text{Li}_3^+$  is not  $\sigma$  aromatic, despite its  $4n + 2$  electron count and negative NICS value.  $\text{H}_3^+$ , with the same valence electron count and a large negative NICS value, is  $\sigma$ -aromatic by virtue of its global ring-current. In the ipsocentric approach, orbital energies and symmetries account for the absence of ring-current in the first system and presence of ring-current in the second. Current mapping proves crucial to understanding the difference in magnetic response between two systems in a case where the magnetic and energetic criteria of aromaticity clearly diverge.

#### Acknowledgements

R.W.A.H. acknowledges financial support from the Netherlands Organisation for Scientific Research (NWO), Grant 700.53.401. F.D.P. and P.G. thank Dr. P.L.A. Popelier for an interesting discussion on Atoms-in-Molecules aspects. P.W.F. is grateful for a Royal Society/Wolfson Research Merit Award.

#### References

- [1] M.J.S. Dewar, *Bull. Soc. Chim. Belg.* 88 (1979) 957.
- [2] D. Cremer, *Tetrahedron* 44 (1988) 7427.
- [3] V.I. Minkin, M.N. Glukhovtsev, B.Y. Simkin, *J. Mol. Struct. (Theochem)* 50 (1988) 93.
- [4] D. Cremer, J. Gauss, *J. Am. Chem. Soc.* 108 (1986) 7467.
- [5] X. Li, A.E. Kuznetsov, H.-F. Zhang, A.I. Boldyrev, L.-S. Wang, *Science* 291 (2001) 859.
- [6] A.E. Kuznetsov, A.I. Boldyrev, X. Li, L.S. Wang, *J. Am. Chem. Soc.* 123 (2001) 8825.
- [7] A.E. Kuznetsov, J.D. Corbett, L.S. Wang, A.I. Boldyrev, *Angew. Chem. Int. Ed.* 40 (2001) 3369.
- [8] P.W. Fowler, E. Steiner, R.W.A. Havenith, *Chem. Phys. Lett.* 342 (2001) 85.
- [9] P.W. Fowler, R.W.A. Havenith, E. Steiner, *Chem. Phys. Lett.* 359 (2002) 530.
- [10] A.I. Boldyrev, A.E. Kuznetsov, *Inorg. Chem.* 41 (2002) 532.
- [11] C.G. Zhan, F. Zheng, D.A. Dixon, *J. Am. Chem. Soc.* 124 (2002) 14795.
- [12] R.W.A. Havenith, P.W. Fowler, E. Steiner, S. Shetty, D. Kanhere, S. Pal, *Phys. Chem. Chem. Phys.* 6 (2004) 285.
- [13] A.N. Alexandrova, A.I. Boldyrev, *J. Phys. Chem. A* 107 (2003) 554.
- [14] A.I. Boldyrev, L.S. Wang, *Chem. Rev.*, to be published.
- [15] B. Twamley, P.P. Power, *Angew. Chem. Int. Ed.* 39 (2000) 3500.
- [16] P. von R. Schleyer, C. Maerker, A. Dransfeld, H. Jiao, N.J.R. van Eikema Hommes, *J. Am. Chem. Soc.* 118 (1996) 6317.
- [17] L. Pauling, *J. Chem. Phys.* 4 (1936) 673.
- [18] F. London, *J. Phys. Radium* 8 (1937) 397.
- [19] J.A. Pople, *J. Chem. Phys.* 24 (1956) 1111.
- [20] P. von R. Schleyer, H. Jiao, *Pure Appl. Chem.* 68 (1996) 209.
- [21] T.A. Keith, R.F.W. Bader, *Chem. Phys. Lett.* 210 (1993) 223.
- [22] T.A. Keith, R.F.W. Bader, *J. Phys. Chem. A* 99 (1993) 3669.
- [23] S. Coriani, P. Lazzeretti, M. Malagoli, R. Zanasi, *Theor. Chim. Acta* 89 (1994) 181.
- [24] R. Zanasi, *J. Chem. Phys.* 105 (1996) 1460.
- [25] E. Steiner, P.W. Fowler, *J. Phys. Chem. A* 105 (2001) 9553.
- [26] E. Steiner, P.W. Fowler, *Chem. Commun.* (2001) 2220.
- [27] GAMESS-UK (2004) is a package of ab initio programs written by M.F. Guest et al. The package is derived from the original GAMESS code, NRCC Software Catalog, vol. 1, Program No. QG01 (GAMESS), 1980.
- [28] P. Lazzeretti et al., *SYSMO Package*, University of Modena, 1980.
- [29] A. Soncini, P.W. Fowler, *Chem. Phys. Lett.* 396 (2004) 174.
- [30] R. Zanasi, P. Lazzeretti, M. Malagoli, F. Piccinini, *J. Chem. Phys.* 102 (1995) 7150.
- [31] R.W.A. Havenith, P.W. Fowler, E. Steiner, *Chem. Eur. J.* 8 (2002) 1068.

- [32] R.F.W. Bader, *Atoms in Molecules – a Quantum Theory*, Oxford University Press, Oxford, 1990.
- [33] A. Sadjadi, M. Abdzadeh, H. Behnejad, *J. Chem. Res.* 5 (2004) 358.
- [34] See e.g. V. Luana, P. Mori-Sanchez, A. Costales, A.M. Pendas, *J. Chem. Phys.* 119 (2003) 6341, and references therein.
- [35] P. Lazzeretti, *Phys. Chem. Chem. Phys.* 6 (2004) 217.